Imaging the Selective Binding of Synapsin to Anionic Membrane Domains

Jill Murray,[a] Louis Cuccia,[a, b] Anatoli Ianoul,[a] James J. Cheetham,[c] and Linda J. Johnston*[a]

Synapsins are membrane-associated proteins that cover the surface of synaptic vesicles and are responsible for maintaining a pool of neurotransmitter-loaded vesicles for use during neuronal activity. We have used atomic force microscopy (AFM) to study the interaction of synapsin I with negatively charged lipid domains in phase-separated supported lipid bilayers prepared from mixtures of phosphatidylcholines (PCs) and phosphatidylserines (PSs). The results indicate a mixture of electrostatic binding to anionic PS-rich domains as well as some nonspecific binding to the PC phase. Interestingly, both protein binding and scanning with synapsin-coated AFM tips can be used to visualize charged lipid domains that cannot be detected by topography alone.

Introduction

Synapsins are neuron-specific peripheral membrane proteins that are associated with the surface of synaptic vesicles. Synapsin I interacts with both protein and lipid components of synaptic vesicles and is believed to tether vesicles to each other and to actin filaments. This maintains a pool of neurotransmitter-loaded vesicles that are used during times of intense neuronal activity. Phosphorylation of the protein acts as a switch to control dissociation of synapsin from actin and vesicles to facilitate neurotransmitter release.[1–3] The interaction of synapsin with membranes has been studied by using synaptic vesicles and liposomes and is hypothesized to be initiated by electrostatic binding to acidic phospholipids.[4–6] Binding induces a conformational change in the protein that is followed by insertion of hydrophobic residues of the N-terminal region into the membrane. We have recently used a combination of surface-pressure measurements for monolayers of neutral and anionic lipids as well as fluorescence studies for vesicles of similar lipid mixtures to study the selective interaction of synapsin with charged lipids.[7] These studies provide evidence for insertion of protein into monolayers of both neutral and zwitterionic lipids at low surface pressure as well as for specific protein interactions with monolayers containing phosphatidylserine (PS) at higher surface pressures that more closely approximate the outer membrane leaflet in synaptic vesicles.

Atomic force microscopy (AFM) has proven to be a useful method for the examination of phase separation of phospholipid monolayers and bilayers on nanometer to micrometer scales under physiological conditions.[8,9] It has also been used to probe the interaction of proteins with supported bilayers and, in particular, to examine the specific interaction of charged proteins with mixtures of zwitterionic and charged lipids.[10–18] For example, annexin has been shown to adsorb to PS-rich membrane domains selectively, in some cases yielding two-dimensional crystalline arrays.[15–18] Similarly, saposin, myelin, and cytochrome C all interact at least partially through electrostatic interactions with bilayers containing charged lipids.[10–12] This work provides information on the role of electrostatic and nonspecific interactions and membrane composition in controlling protein adsorption on lipid bilayers and also yields insight into protein-mediated membrane disruption.

In order to provide more direct evidence for the interaction of synapsin with anionic membrane domains, we have used AFM and near-field scanning optical microscopy (NSOM)[19–22] to image supported lipid bilayers comprised of mixtures of neutral phosphatidylcholine (PC) and anionic PS lipids. This allows the direct visualization of both specific and nonspecific protein binding, depending on the composition of the bilayer. In the course of these studies, we observed that synapsin-coated AFM tips can be used to visualize PS-rich regions of supported bilayers that cannot be detected by topography alone. These results, in combination with other studies of AFM imaging of supported synaptic vesicles,[23–25] provide a basis on which to design an in vitro model for some of the key steps involved in binding synapsin vesicles to each other and to actin fibers and for probing the interaction of synaptic vesicles with membranes.

Results and Discussion

PC/PS bilayers in the presence and absence of synapsin I

Hybrid bilayers with dipalmitoyl phosphatidylethanolamine (DPPE) as the lower leaflet and PC/DPPS (DPPS, dipalmitoyl

[a] *J. Murray, Prof. L. Cuccia, Dr. A. Ianoul, Dr. L. J. Johnston*
Steacie Institute for Molecular Sciences, National Research Council Canada
100 Sussex Drive, Ottawa, Ontario, K1A 0R6 (Canada)
Fax: (+1) 613-952-0068
E-mail: linda.johnston@nrc-cnrc.gc.ca

[b] *Prof. L. Cuccia*
Current address:
Department of Chemistry and Biochemistry, Concordia University
7141 Sherbrooke Street West, Montréal, Québec, H4B 1R6 (Canada)

[c] *Prof. J. J. Cheetham*
Department of Biology, Carleton University
1125 Colonel By Drive, Ottawa, Ontario, K1S 5B6 (Canada)

 DOI: 10.1002/cbic.200400097

phosphatidylserine) mixtures as the top leaflet were prepared by successive transfer of two monolayers from the air–water interface. DPPE monolayers were transferred to mica at a pressure of 40 mN m^{-1}, since previous work had shown this to give the best results for transfer of a second monolayer.[13] The upper leaflets contained mixtures of 20 mol% DPPS with either C_{12} or C_{16} phosphatidylcholines and were transferred at pressures between 30 and 40 mN m^{-1}. Figure 1 shows AFM images for the two PC/DPPS (4:1) bilayers in water; the use of 20% charged lipid was based on the estimated percentage of charged lipids in the cytoplasmic leaflet of synaptic vesicle membranes.[26] The DPPC/DPPS bilayer (Figure 1A; DPPC, dipalmitoyl phosphatidylcholine) appears uniformly flat with only occasional small dots of debris on the surface. This is consistent with previous results demonstrating that Ca^{2+} or the protein annexin are required to visualize domains by AFM for DPPC/DPPS bilayers prepared by Langmuir–Blodgett transfer.[18,27] By contrast, bilayers with DLPC/DPPS (4:1; DLPC, dilauroyl phosphatidylcholine) as the top leaflet showed clear phase separation (Figure 1B). The image shows large irregularly shaped domains that are approximately 1.5 nm higher than the surrounding phase and which we assign to DPPS-rich regions. The relative area covered by these domains varies between 10 and 25%, depending on the area imaged; this might indicate that the raised domains contain some DLPC. Smaller scale images (Figure 1C and D) show that the lower phase contains a substantial number of small holes or defects and that there are also a few similar holes in the large PS-rich domains. The apparent depth of these "holes" increases with small increases in imaging force (compare Figure 1C and D; the holes are barely visible in the latter image). This suggests that they might be small disordered domains that are much easier for the tip to penetrate than the bulk surrounding phase. We have observed similar effects when imaging small negatively charged glycolipid domains in supported bilayers.[13]

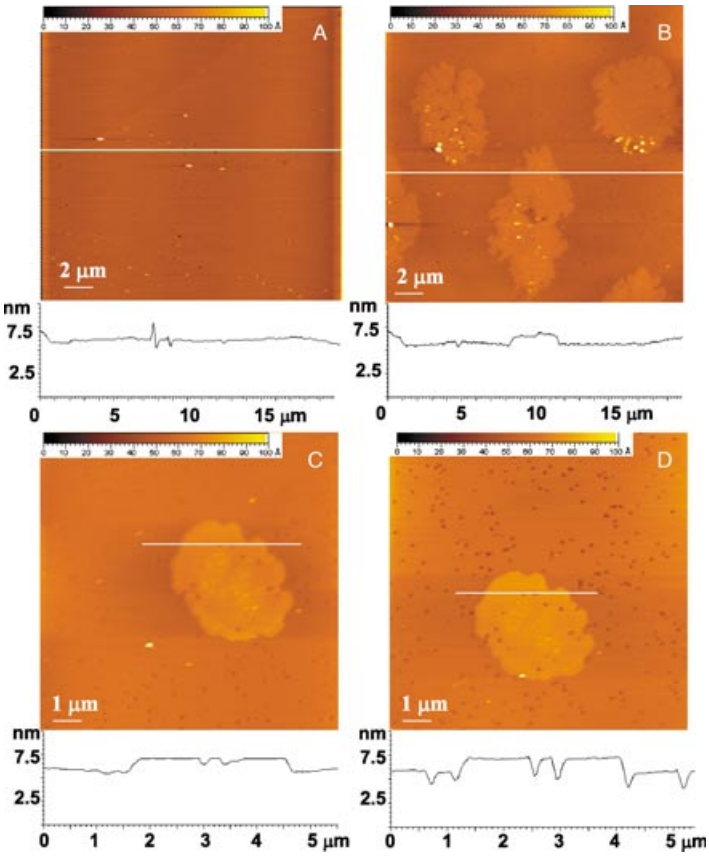

Figure 1. AFM images of PC/DPPS (4:1) on DPPE bilayers (A, DPPC; B–D, DLPC) in water. Images C and D were imaged at higher and lower force, respectively.

We examined the effect of calcium on PC/PS bilayers since several previous studies have indicated that the presence of calcium results in changes in the bilayer's morphology.[17,27] No significant changes were observed for DLPC/DPPS (4:1) on DPPE bilayers when the initial bilayer was formed in the presence of buffer containing Ca^{2+} or when Ca^{2+} was added to a preformed bilayer. This contrasts with previous results for DPPC/DOPS (DOPS = dioleoylphosphatidylserine) bilayers, which showed changes in domain size and shape in the presence of calcium.[17] However, it is consistent with the fact that the difference in chain length for DLPC versus DPPS will favor phase separation, independent of the presence of calcium.

Images of the DLPC/DPPS bilayer shown in Figure 1B–D after incubation with synapsin are shown in Figure 2. The PS-rich domains are approximately 4–5 nm higher than the surrounding fluid phase as compared to only 1.5 nm in the absence of protein (compare Figures 1B and 2A for the same scan size); this is consistent with protein binding to the PS domains. There are also many small raised dots scattered randomly throughout the lower DLPC phase. Smaller images (Figure 2B) show that these domains are approximately 3–4 nm in height and that the small holes or defects observed in the bilayer before protein incubation are no longer visible. This suggests that protein binds to the small defects or disordered islands in the DLPC phase. After protein addition the measured heights are not sensitive to imaging force, at least over the same range of forces that leads to quite pronounced changes

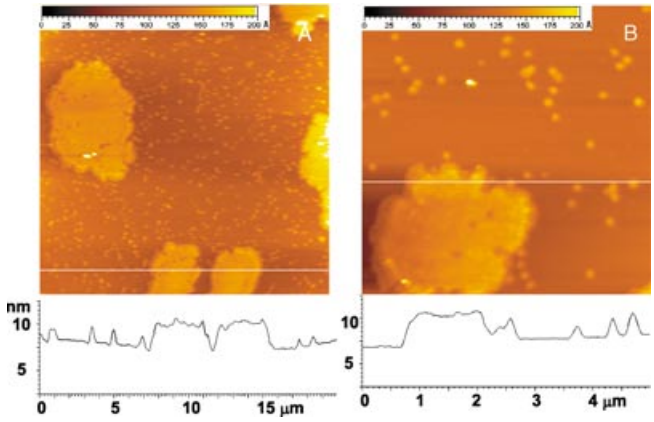

Figure 2. AFM images of a DLPC/DPPS (4:1) on DPPE bilayer after incubation with synapsin I and rinsing with water.

in the apparent depth of the defects observed in the absence of protein. The small-scale image demonstrates that the protein distribution is not completely uniform across the large domains, since there are occasional small brighter dots clustered around the domain boundaries (Figure 2B).

DPPC/DPPS bilayers were also incubated with synapsin. Although bilayers in the absence of protein showed little evidence of phase separation, as described above, incubation with protein resulted in large round domains that were 5–7 nm above the surrounding phase (Figure 3A and B). We infer by analogy to the results for DLPC/DPPS bilayers that these are again PS-rich domains. In some cases there appeared to be a preference for protein binding around the edges of the large domains. In addition to the large domains there are many small raised dots on the bilayers after protein incubation; these are 200–250 nm in diameter and 15 nm high. A control experiment with a DPPC on DPPE bilayer before and after incubation with synapsin is shown in Figure 3C and D. The same small raised dots are observed after protein incubation; this is consistent with nonspecific binding of protein to the PC phase of the bilayers. However, it is interesting to note that the nonspecific adsorption appears to lead only to small microdomains, whereas binding to PS domains gives reasonably uniform coverage over a much larger area. Synapsin, which was centrifuged to remove aggregates, gave similar results; this indicates that the small dots of protein were not due to protein oligomers in solution.

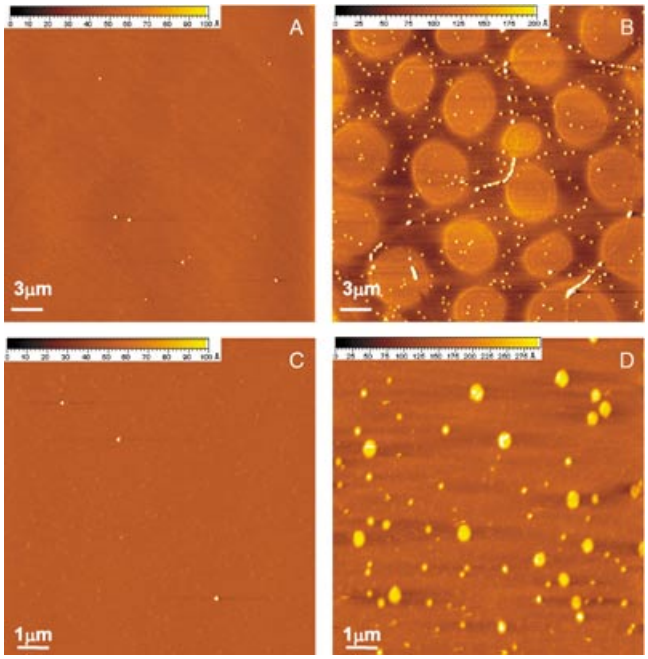

Figure 3. *AFM images of a DPPC/DPPS (4:1) on DPPE (A, B) and a DPPC on DPPE bilayer (C, D) before (A, C) and after (B, D) incubation with synapsin I and rinsing with water.*

Use of synapsin-coated tips to visualize anionic domains

Our initial experiments with synapsin binding to DPPC/DPPS bilayers led to the interesting discovery that a tip that had previously been used to image a sample containing synapsin can then be used to observe clear contrast for DPPC/DPPS bilayers that appear uniformly flat when imaged with a new tip. This prompted us to image a DPPC/DPPS bilayer and then expose the tip to a solution of synapsin for approximately an hour prior to using it to reimage the same bilayer. As shown in Figure 4A and B, domains are readily visible after the tip has been incubated in protein solution. They are similar in size and shape to those observed upon protein binding. This indicates that the protein-coated tip interacts quite differently with PS versus PC areas of the bilayers, allowing visualization of domains that do not show up in a topographic scan with an uncoated tip. It is also interesting to note that Figure 4B shows no evidence for the small dots of protein observed in Figure 3B and D; this clearly demonstrates that they arise from nonspecific binding of synapsin to the PC phase of the bilayer.

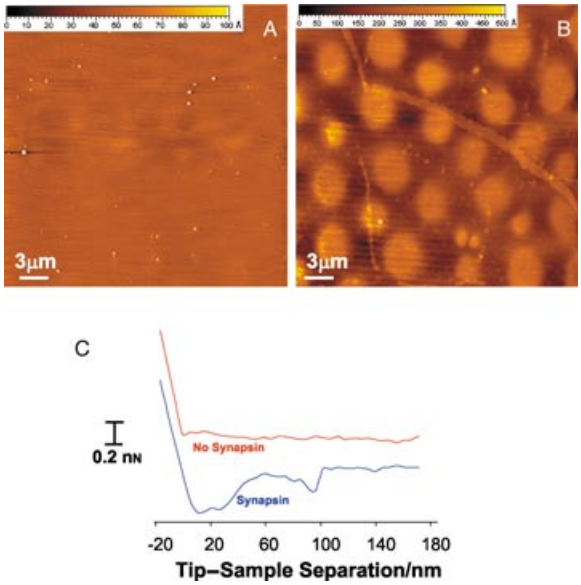

Figure 4. *AFM images of a DPPC/DPPS (4:1) on DPPE bilayer imaged with an A) uncoated and B) synapsin-coated tip. The force–distance curves measured for retraction of an uncoated and a synapsin-incubated tip from a DPPC/DPPS bilayer are shown in C.*

Force measurements were used to examine the tip–surface interaction in more detail. Figure 4C shows a comparison of the force–distance curves for the retraction trace on a DPPC/DPPS bilayer for a silicon nitride tip before and after incubation with synapsin. The force curve for the protein-coated tip was measured for a raised domain and reveals a series of adhesive jumps that are not observed in the absence of protein. This is consistent with electrostatic interaction of the positively charged protein with negatively charged PS domains of the bilayer. The observation of multiple adhesive jumps is consistent with literature data for force measurements with protein ad-

sorbed on or covalently attached to tips and for interaction of tips with proteins on surfaces.[10,28–30] The multiple jumps are generally attributed to a convolution of multiple unbinding or unfolding processes. However, it should be noted that interpretation of the data is more straightforward in cases in which the protein is covalently attached to the tip. In the present experiments, we cannot exclude the possibility that there is equilibration of the protein between the tip and the bilayer during our experiment. Detailed force studies with covalently modified tips would be required to provide a more detailed understanding of the image contrast and force curves that we observe for the synapsin-modified tips. Nevertheless, the results clearly demonstrate that adsorption of synapsin on the tip occurs very readily under our usual imaging conditions. In fact, it is likely that in all cases the images that we measure in the presence of synapsin reflect some level of synapsin-tip contamination; the apparent heights therefore reflect a combination of topography and specific tip–sample interactions.

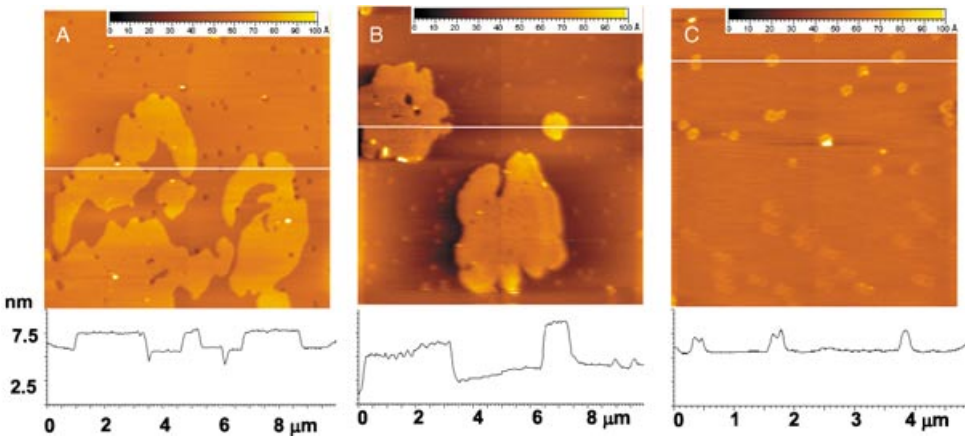

Figure 5. *AFM images of a DLPC/DPPS (4:1) on DPPE bilayer measured with an A) uncoated and B), C) synapsin-coated tip.*

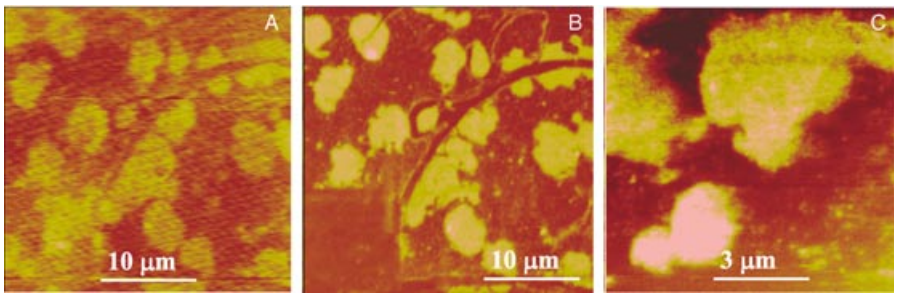

Figure 6. *NSOM images of a DLPC/DPPS (4:1) on a DPPE bilayer incubated with synapsin I–Alexa-488. A) topography; B), C) fluorescence. Image B was recorded after image C and shows the rapid bleaching (bottom left corner correspond to the area imaged for C) induced by the near field probe.*

The DLPC/DPPS bilayers were also imaged with a synapsin-coated tip. In this case the apparent height of the domains was considerably larger after the tip had been exposed to synapsin, as shown in Figure 5 A and B. Of particular interest is the fact that the small defects observed in the DLPC phase of the bilayer (Figure 5 A) now appear as raised areas (Figure 5 C). This further confirms that these areas contain PS and are not simply holes in one or both leaflets of the bilayer.

The images obtained with synapsin-coated tips are qualitatively similar to those obtained by incubating bilayers with synapsin. To eliminate any uncertainty in assessment of the apparent height changes in the AFM images for samples incubated with synapsin, we have used NSOM to verify the binding of synapsin to anionic domains. Figure 6 shows topographic and fluorescence images for a DLPC/DPPS bilayer incubated with Alexa-488-labeled synapsin. Large fluorescent synapsin-covered domains are visible as higher areas in the topographic image (Figure 6 A) and as brighter areas in the optical image (Figure 6 B and C). These clearly correspond to the same protein-covered PS domains observed by AFM. The fluorescence images indicate uniform coverage of the PS domains with protein, at least at the resolution of the NSOM experiments (limited by the 150 nm probe aperture). A small-scale NSOM image (Figure 6 C) also shows the small microdomains that are observed by AFM. The dye-labeled protein bleaches rapidly under the conditions of the NSOM experiment. Figure 6 C was measured first and then the same area was reimaged on a larger scale (Figure 6 B). The small dark area in the lower left corner corresponds to the area imaged in Figure 6 C, indicating that the dye has been almost completely photobleached. Although this level of photobleaching is problematic for multiple scans of the same area, it does clearly show that the optical contrast observed cannot arise from topography-induced artifacts.[31]

Conclusion

The AFM and NSOM images presented above allow direct visualization of the selective binding of synapsin I to anionic bilayer domains and are in good agreement with earlier reports on the interaction of synapsin with negatively charged lipids. In addition to specific binding mediated by electrostatic interactions there is also some nonspecific binding to the PC-rich phase of the bilayers. This appears to be more pronounced for gel-phase DPPC than for fluid DLPC membranes, since most of the small protein islands observed for DLPC mixtures result

from specific binding to PS microdomains, rather than nonspecific binding. The combination of specific electrostatic interactions and nonspecific binding has also been observed previously upon binding of charged proteins, such as myelin and cytochrome C, to supported membranes.[10] Interestingly, the present results indicate that synapsin-coated tips facilitate the visualization of charged bilayer domains that are not detected by topography alone. The measured force curves for such tips are consistent with multiple protein–lipid binding interactions and may also reflect some equilibration of the protein between the negatively charged tip and lipid. The enhanced contrast obtained with protein-coated tips may provide a general tool for understanding the membrane distribution of charged lipids.

In addition to allowing the direct visualization of the interaction between synapsin and charged lipid domains, the supported membranes can be used as an in vitro model for the surface of synaptic vesicles that have a large amount of adsorbed protein. AFM images provide evidence for a nonuniform protein distribution on the charged PS domains and synapsin clearly does not give a regular two-dimensional crystalline layer, as has been observed for annexin on fluid PC/PS bilayers.[15–18] Furthermore, the curvature of small synaptic vesicles may lead to a different packing and arrangement of protein on the surface than that obtained for planar lipid bilayers. The small clusters observed around the edges of the PS domains in some images may reflect protein oligomerization since synapsin is known to undergo both homo and heterodimerization.[32] Note that the present results do not allow us to distinguish between electrostatic interactions and insertion of hydrophobic synapsin residues into the bilayer. However, based on our previous surface-pressure results it is likely that the specific electrostatic interaction of synapsin with charged lipids is followed by insertion into the membrane.[7]

Experimental Section

Sample preparation: Dipalmitoyl phosphatidylcholine (DPPC), dilauroyl phosphatidylcholine (DLPC), dipalmitoyl phosphatidylethanolamine (DPPE), and dipalmitoyl phosphatidylserine (DPPS) were purchased from Avanti Polar Lipids, Alabaster, AL. Synapsin I was purified from bovine brain under nondenaturing conditions, as previously described, and its purity checked by SDS-PAGE.[33,34] The protein was stored in buffer (100 mM NaCl, 25 mM Tris-HCl, pH 7.4) at −80 °C. Synapsin I was labeled with Alexa-488 by using a Molecular Probes protein labeling kit and following the manufacturer's directions for labeling and purification. The degree of labeling was estimated to be approximately one dye/protein, based on the absorbance at 280 and 494 nm.

Monolayers and bilayers were prepared on a Langmuir–Blodgett trough (NIMA 611, Coventry, UK) by using Milli-Q water as the subphase. The sample solution in chloroform was spread on the subphase surface; after solvent evaporation (10 min) the monolayer was compressed at 20 $cm^2 min^{-1}$ to the desired surface pressure, measured with a precision of 0.1 $mN m^{-1}$ by using a Wilhelmy balance. Monolayers were expanded and recompressed at least twice to anneal the sample before transfer to a freshly cleaved, hydrophilic 2.5 cm^2 mica sheet by vertical deposition with a dipping speed of 2 $mm min^{-1}$. Transfer ratios of 85–100% were typical. Bilayers were prepared by transferring a second monolayer to mica coated with a lipid monolayer. The second monolayer was also annealed twice before transferring. The resulting bilayers were transferred under water in a small container during the transfer to the AFM liquid cell (Molecular Imaging Inc.). Bilayers were incubated with protein by adding protein (10–50 μL, 0.5 $mg mL^{-1}$) to water (0.5 mL) in the AFM fluid cell, followed by rinsing with water to remove unbound protein.

Atomic force microscopy: AFM measurements for bilayer samples were carried out on a Picoscan atomic force microscope (Molecular Imaging, MI) in the repulsive mode or in Mac mode.[35] In contact mode, silicon nitride tips with spring constants of ~60 $mN m^{-1}$ were used. The force curves were obtained in contact mode by using the force spectroscopy feature of the MI microscope. The imaging force was calibrated by recording a force curve on a hard surface (test pattern). The imaging force was minimized to ~1 nN. Magnetic coated silicon tips with spring constants of 0.5 $N m^{-1}$ and resonance frequencies between 25 and 40 kHz in aqueous solution were used for Mac-mode measurements. The drive voltage was normally around 15 mV. Scanners with maximum scan areas of 30×30 and 5×5 μm^2 were used. For experiments with synapsin-coated tips, tips were incubated in the synapsin solution (0.5 $mg mL^{-1}$, water) for 30 min. Although both contact and Mac-mode imaging were used, all images shown in the figures were obtained by using Mac mode since this gave better results, particularly for protein samples.

Near-field scanning optical microscopy: Bent NSOM probes were prepared from high GeO_2-doped fibers with a core diameter of 3 μm by using a two-step chemical-etching method followed by aluminum deposition and focused ion-beam milling to produce the aperture.[22] Probes with an aperture diameter of 100–150 nm and an estimated spring constant of ~100 $N m^{-1}$ were used in the present work.[22]

NSOM experiments were carried out on a combined AFM/NSOM microscope based on a Digital Instruments Bioscope mounted on an inverted fluorescence microscope (Zeiss Axiovert 100), as described previously.[21] A continuous-wave mixed-gas ion laser (Coherent, Innova 70 Spectrum) was used for excitation purposes (488 nm, 20–30 mW). Fluorescence was collected with a 40× objective (0.7 NA), with appropriate filters to remove residual excitation (488 nm notch filter, Kaiser Optical Systems, Ann Arbor, MI) and red alignment laser light (Chroma 670 nm cut-off filter, Brattleboro, VT), and detected by using an avalanche photodiode detector (Perkin Elmer Optoelectronics, SPCM-AQR-15, Vaudreuil, Canada). For imaging in liquid, a two-step approach was used: approach to the water surface and approach to the sample surface.[21] During imaging only a fraction of the tip (~0.5 mm) was immersed in liquid, while the rest was kept in air. Images were recorded in tapping mode at a scan rate of 0.5 Hz and a resolution of 256× 256.

Keywords: AFM · membrane proteins · membranes · near-field scanning optical microscopy · vesicles

[1] S. Hilfiker, V. S. Pieribone, A. J. Czernik, H.-T. Kao, G. J. Augustine, P. Greengard, *Phil. Trans. R. Soc. Lond. B* **1999**, *354*, 269–279.
[2] M. Hosaka, R. E. Hammer, T. C. Sudhof, *Neuron* **1999**, *24*, 377–387.
[3] P. Chi, P. Greengard, T. A. Ryan, *Nat. Neurosci.* **2001**, *4*, 1187–1193.
[4] G. Stefani, F. Onofri, F. Valtorta, P. Vaccaro, P. Greengard, F. Benfenati, *J. Physiol.* **1997**, *504*, 501–515.

[5] J. J. Cheetham, S. Hilfiker, F. Benfenati, T. Weber, P. Greengard, A. J. Czernik, *Biochem. J.* **2001**, *354*, 57 – 66.
[6] F. Benfenati, F. Valtorta, M. C. Rossi, F. Onofri, T. Sihra, P. Greengard, *J. Cell. Biol.* **1993**, *123*, 1845 – 1855.
[7] J. C. Cheetham, J. Murray, M. Ruhkalova, L. Cuccia, R. McAloney, K. U. Ingold, L. J. Johnston, *Biochem. Biophys. Res. Commun.* **2003**, *309*, 823 – 829.
[8] Y. F. Dufrene, G. U. Lee, *Biochim. Biophys. Acta* **2000**, *1509*, 14 – 41.
[9] A. Janshoff, C. Steinem, *ChemBioChem* **2001**, *2*, 798 – 808.
[10] H. Mueller, H.-J. Butt, E. Bamberg, *J. Phys. Chem.* **2000**, *104*, 4552 – 4559.
[11] H. X. You, L. Yu, X. Qi, *FEBS Lett.* **2001**, *503*, 97 – 102.
[12] H. X. You, X. Qi, G. A. Grabowski, L. Yu, *Biophys. J.* **2003**, *84*, 2043 – 2057.
[13] C. Yuan, L. J. Johnston, *Biophys. J.* **2001**, *81*, 1059 – 1069.
[14] C. Yuan, J. Furlong, P. Burgos, L. J. Johnston, *Biophys. J.* **2002**, *82*, 2526 – 2535.
[15] I. Reviakine, W. Bergsma-Schutter, A. N. Morozov, A. Brisson, *Langmuir* **2001**, *17*, 1680 – 1686.
[16] I. Reviakine, W. Bergsma-Schutter, A. Brisson, *J. Struct. Biol.* **1998**, *121*, 356 – 361.
[17] I. Reviakine, A. Simon, A. Brisson, *Langmuir* **2000**, *16*, 1473 – 1477.
[18] A. Janshoff, M. Ross, V. Gerke, C. Steinem, *ChemBioChem* **2001**, *2*, 587 – 590.
[19] P. F. Barbara, D. M. Adams, D. B. O'Connor, *Ann. Rev. Mater. Sci.* **1999**, *29*, 433 – 469.
[20] R. C. Dunn, *Chem. Rev.* **1999**, *99*, 2891 – 2928.
[21] A. Ianoul, P. Burgos, Z. Lu, R. S. Taylor, L. J. Johnston, *Langmuir* **2003**, *19*, 9246 – 9254.
[22] P. Burgos, Z. Lu, A. Ianoul, C. Hnatovsky, M.-L. Viriot, L. J. Johnston, R. S. Taylor, *J. Microscopy* **2003**, *211*, 37 – 47.
[23] R. A. Garcia, D. E. Laney, S. M. Parsons, H. G. Hansma, *J. Neurosci. Res.* **1998**, *52*, 350 – 355.
[24] D. E. Laney, R. A. Garcia, S. M. Parsons, H. G. Hansma, *Biophys. J.* **1997**, *72*, 806 – 813.
[25] V. Parpura, R. T. Doyle, T. A. Basarsky, E. Henderson, P. G. Haydon, *Neuroimage* **1995**, *2*, 3 – 7.
[26] E. W. Westhead, *Ann. NY Acad. Sci.* **1987**, *493*, 92 – 99.
[27] M. Ross, C. Steinem, H.-J. Galla, A. Janshoff, *Langmuir* **2001**, *17*, 2437 – 2445.
[28] E.-L. Florin, V. T. Moy, H. E. Gaub, *Science* **1994**, *264*, 415 – 417.
[29] K. Feldman, G. Hahner, N. D. Spencer, P. Harder, M. Grunze, *J. Am. Chem. Soc.* **1999**, *121*, 10 134 – 10 141.
[30] S. Kidoaki, T. Matsuda, *Langmuir* **1999**, *15*, 7639 – 7646.
[31] B. Hecht, H. Bielefeldt, Y. Inouye, D. W. Pohl, *J. Appl. Phys.* **1997**, *81*, 2492 – 2498.
[32] M. Hosaka, T. C. Sudhof, *J. Biol. Chem.* **1999**, *274*, 16 747 – 16 753.
[33] W. Schiebler, R. Jahn, J. P. Doucet, J. Rothlein, P. Greengard, *J. Biol. Chem.* **1986**, *261*, 8383 – 8390.
[34] M. Bahler, P. Greengard, *Nature* **1987**, *326*, 704 – 707.
[35] W. Han, S. M. Lindsay, T. Jing, *Appl. Phys. Lett.* **1996**, *69*, 4111 – 4114

Received: April 6, 2004
Early View Article
Published online on October 13, 2004

